

Inorganic carbon fluxes through the boundaries of the Greenland Sea Basin based on in situ observations and water transport estimates

Melissa Chierici ^{a,*}, Helge Drange ^b, Leif G. Anderson ^a, Truls Johannessen ^c

^a Department of Analytical and Marine Chemistry, Göteborg University, SE-412 96 Göteborg, Sweden

^b Nansen Environmental and Remote Sensing Center, Edward Griegs vei 3a, N-5037 Solheimsviken, Bergen, Norway

^c Department of Geophysics, University of Bergen, Allegaten 70, N-5007 Bergen, Norway

Received 30 November 1998; accepted 21 May 1999

Abstract

A carbon budget for the exchange of total dissolved inorganic carbon C_T between the Greenland Sea and the surrounding seas has been constructed for winter and summer situations. An extensive data set of C_T collected over the years 1994–1997 within the European Sub-polar Ocean Programmes (ESOP1 and ESOP2) are used for the budget calculation. Based on these data, mean values of C_T in eight different boxes representing the inflow and outflow of water through the boundaries of the Greenland Sea Basin are estimated. The obtained values are then combined with simulated water transports taken from the ESOP2 version of the Miami Isopycnic Coordinate Ocean Model (MICOM). The fluxes of inorganic carbon are presented for three layers; a surface mixed layer, an intermediate layer and a deep layer, and the imbalance in the fluxes are attributed to air–sea exchange, biological fixation of inorganic carbon, and sedimentation. The main influx of carbon is found in the surface and the deep layers in the Fram Strait, and in the surface waters of direct Atlantic origin, whereas the main outflux is found in the surface layer over the Jan Mayen Fracture Zone and the Knipovich Ridge, transporting carbon into the Atlantic Ocean via the Denmark Strait and towards the Arctic Ocean via the Norwegian Sea, respectively. The flux calculation indicates that there is a net transport of carbon out of the Greenland Sea during wintertime. In the absence of biological activity, this imbalance is attributed to air sea exchange, and requires an oceanic uptake of CO_2 of $0.024 \pm 0.006 \text{ Gt C yr}^{-1}$. The flux calculations from the summer period are complicated by biological fixation of inorganic carbon, and show that data on organic carbon is required in order to estimate the air–sea exchange in the area. © 1999 Elsevier Science B.V. All rights reserved.

Keywords: air–sea exchange; Greenland Sea; inorganic carbon

1. Introduction

The oceanic carbon cycle and its role in the uptake, transport and mixing of carbon dioxide originating from burning of fossil fuels, cement production, and change in the use of land is a key issue regarding problems related to climate change. Esti-

* Corresponding author. Tel.: +46-31-772-2777; Fax: +46-31-772-2785; E-mail: melissa@amc.chalmers.se

mates based on numerical box and Ocean General Circulation Models (OGCMs) suggest that about one-third of the anthropogenic carbon dioxide emissions are absorbed by the global oceans within 2–5 years (Maier-Reimer and Hasselmann, 1987; Sarmiento et al., 1992). However, it is difficult to compare the model results with in situ observations as anthropogenic carbon dioxide is only a small fraction of the total dissolved inorganic carbon concentration in seawater (typically up to about 40 of 2100 $\mu\text{mol kg}^{-1}$), and it cannot be distinguished chemically except for the ^{13}C - and ^{14}C -dilution effects (Suess, 1955; Quay et al., 1992).

Methods have been presented where the measured concentration of total dissolved inorganic carbon (C_T) is corrected for different biochemical processes, as well as for the time since it was in contact with the atmosphere, by use of other measured tracers (Gruber et al., 1996; Anderson et al., 1998a). The estimated ocean uptake using these methods agree, within the uncertainty of the measurements, with the estimates based on OGCMs (e.g., Siegenthaler and Sarmiento, 1993). One of the common results from these investigations and also from direct measurements of the partial pressure of carbon dioxide ($p\text{CO}_2$) in surface water (e.g., Takahashi et al., 1993, 1995) is that the high latitude oceans are one of the strongest sink regions of atmospheric CO_2 , at least per unit area. There are several reasons for this, including cooling of the surface water with a simultaneous increase in the solubility of carbon dioxide, that the wind speed is generally high, especially during the winter months, and that subsurface waters are formed here by means of deep mixing and convection.

The most significant deep water production area north of the Greenland Scotland Ridge is probably the Greenland Sea. The deep and intermediate water produced north of this ridge is one of the components in the bottom water that flows southward into the North Atlantic (Dickson and Brown, 1994), and this overflow can be viewed as the northern limb of the Global Thermohaline Circulation (Broecker, 1991). Hence, the flux of carbon in the Greenland Sea may also have some significance in the global cycling of carbon.

The Greenland Sea is situated between the northward flowing warm and saline Norwegian Atlantic

Current and the southward flowing cold and fresh East Greenland Current (Meincke, 1983; Buch et al., 1988). The East Greenland Current transports water out of the Arctic Ocean and cover a depth range of more than 2000 m (e.g., Aagaard et al., 1991). Most of the water follows the continental margin along the western rim of the Greenland Basin, but some is mixed into the Greenland Sea gyre. The Norwegian Atlantic Current, on the other hand, is fairly shallow (covers the uppermost 500 to 1000 m of the water column), and while a part continues into the Arctic Ocean, the rest recirculates in the northern Greenland Sea and in the Fram Strait region. In fact, it is the Norwegian Atlantic Current that supplies salt (possibly together with brine released from formation of sea ice) that is needed to increase the density to form deep water in the Greenland Sea. The deep water formed is then mixed with outflowing Arctic Ocean Deep Water, forming Norwegian Sea Deep Water (Swift and Koltermann, 1988). Some of the produced Norwegian Sea Deep Water is flowing north into the Arctic Ocean, while the rest is believed to spill through the gaps in the Knipovich Ridge into the Norwegian Sea.

The magnitude of the deep water formation is variable and a significant decrease since the early 1980s has been observed (Schlosser et al., 1991; Bönisch et al., 1997). Nevertheless, the overflow volume into the North Atlantic, between Iceland and Greenland, has been shown to be relatively constant (Dickson and Brown, 1994). It should be noted that the Denmark Strait overflow time series only covers some years, and it is therefore not possible to evaluate if the magnitude of the overflow varies on the decadal time scales characteristic of the North Atlantic Oscillation (Hurrell, 1995).

In this work, we couple measured concentrations of C_T with flow estimates simulated by an OGCM. The reason for using simulated flow transports are based on the fact that flow transports in the region are poorly known, and that an OGCM gives a consistent flow field due to conservation of basic fluid dynamic properties like mass, salt, heat, momentum, and various forms of energy.

The goals of the work are three-fold: (i) to achieve the total inorganic carbon fluxes between the Greenland Sea and surrounding waters for the winter season, making it possible to elucidate the air–sea

exchange of the region for that period of the year; (ii) to obtain an estimate of the net sink of total inorganic carbon (air–sea exchange plus biological fixation) during the summer period; and (iii) to identify uncertainties and ways to improve the accuracy of the obtained results.

2. Definition of the Greenland Sea

In this study, we have defined the boundaries of the Greenland Sea according to the main topographic

features in the area. The boundaries displayed in Fig. 1 would therefore coincide with the current systems in the region if topographic steering was the major constraint on the dynamics. In the following, *inflow* represents the flow of water into the Greenland Sea

- across the Mohn's Ridge from 71°N, ~20°W to 73.5°N, 7°E (boundary 1),
- across the Knipovich Ridge from 73.5°N to 78.5°N along 7°E (boundary 2),
- across the Fram Strait at 78.5°N from 7°E to 20°E (boundary 3), and

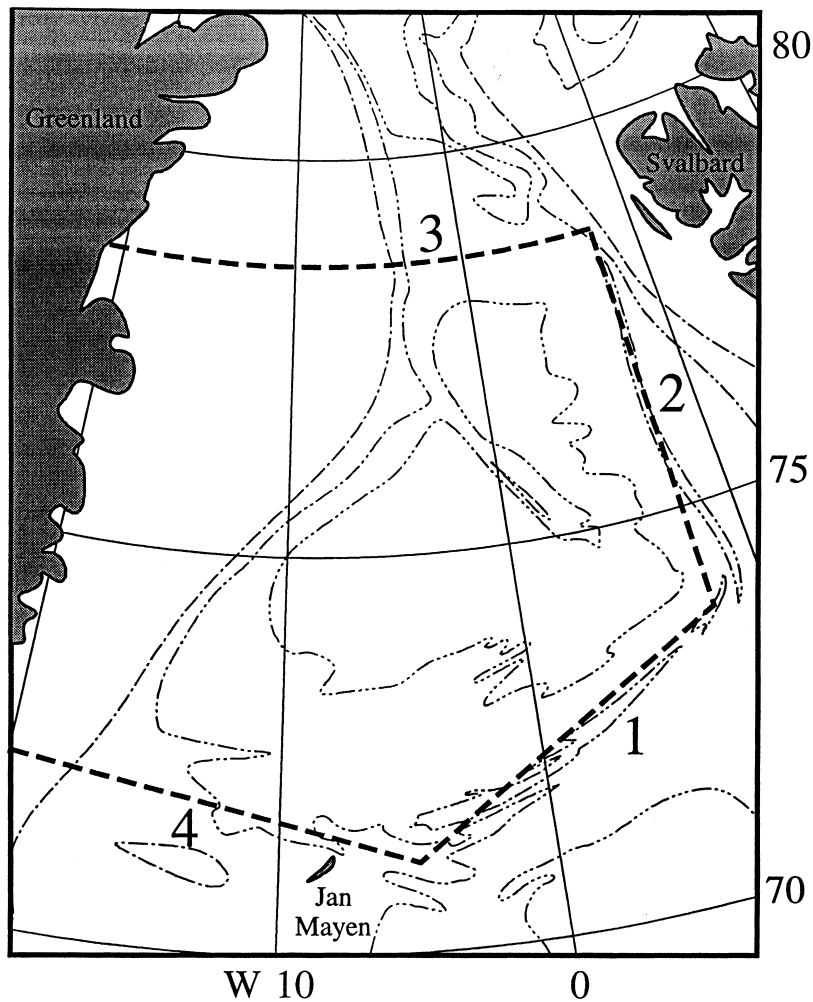


Fig. 1. The investigated area and the surrounding seas are shown. The area within the stretched lines represents the study area and the four boundaries are shown as dashed lines.

- between Jan Mayen and Greenland from 72°N, ~ 20°W to 71°N, 5°W (boundary 4).

The coast of Greenland is taken as the western boundary of the Greenland Sea.

3. The circulation model

Estimates of the water transport in and out of the Greenland Sea as defined above can be obtained in several ways; directly deduced from hydrography and/or flow observations (diagnostic approach), by using inverse models of various complexity constrained by hydrography and tracer observations, or by prognostic OGCM. In this study, the ESOP2 version (Drange and Simonsen, 1997a,b; Simonsen and Drange, 1997) of the fully prognostic MICOM (Bleck et al., 1992) has been used to determine the water transports in and out of the Greenland Sea region.

MICOM is an ocean general circulation model which utilizes surfaces of constant density (isopycnal surfaces) as the vertical coordinate. In the configuration used here, the reference pressure is set to zero, and the layer densities are expressed in σ_θ -units. In the present version of the ESOP2 model, there are 14 isopycnal layers with prescribed σ_θ -limits of 26.2, 26.8, 27.25, 27.55, 27.75, 27.86, 27.93, 27.98, 28.01, 28.03, 28.05, 28.07, 28.08, and 28.09, and a mixed layer of variable density at the top of the water column. The model domain covers the Atlantic Ocean from about 20°S and northwards, including the Arctic Ocean. A dynamic–thermodynamic sea ice model has been coupled to the ocean circulation model. The horizontal grid system is local orthogonal with grid focus in the Nordic Seas. The horizontal resolution in the focus region vary from 55 to 65 km, whereas the grid spacing is about 250 km near the southern and northern model borders. The model topography is realistic and for each model grid cell, the ocean

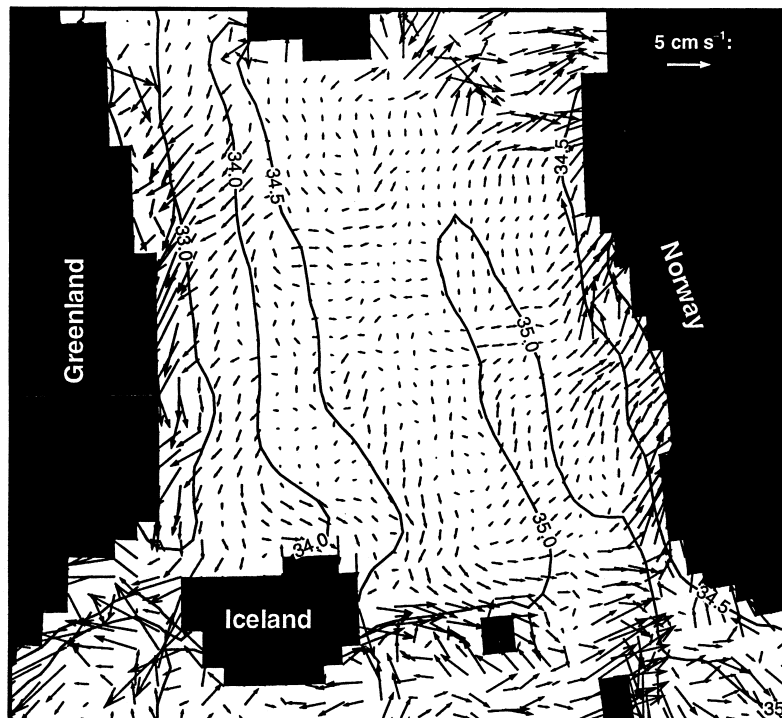


Fig. 2. The vertically integrated velocity field, together with the mean SSS field, averaged from January to March, simulated by the ESOP2 of the MICOM model.

depth equals the arithmetic mean of a 5-min resolution topography data base.

The circulation model is initialized by observed hydrography (Levitus and Boyer, 1994; Levitus et al., 1994), and spun up from rest. As forcing fields, climatological or monthly mean 10 m wind (ECMWF, 1988), 2 m surface air temperature (ECMWF, 1988; Simonsen and Haugan, 1996), cloudiness (Huschke, 1969; Oberhuber, 1988), precipitation (Legates and Willmott, 1990), and relative humidity (Maykut, 1978; Oberhuber, 1988) are used. The sea surface salinity (SSS) and sea surface temperature (SST) fields are relaxed towards observed monthly mean SSS and SST (Levitus et al., 1994) with a relaxation time scale of one month for a 100 m deep mixed layer (New et al., 1995).

For the first 5 years, the ocean dynamics and thermodynamics evolve according to inconsistencies between the initial density structure and the applied surface forcing. After an integration time of about 10

years, the evolution of the simulated dynamics and thermodynamics approaches an annually repeated cycle. The simulated fields used in this study have been extracted as monthly mean mass transport and layer thickness fields for each of the boundaries from model year 15. In addition, the monthly mean ice covered area in the Greenland Sea region was extracted.

A thorough description of the simulated dynamic and thermodynamic fields is beyond the scope of the present paper. However, the surface water velocity field, together with the simulated SSS at the beginning of January are shown in Fig. 2. The major current systems are in general agreement with the large scale circulation of the Nordic Seas (Nansen, 1906; Johannessen, 1986; Hopkins, 1991), with the exception that the net southward transport of water through the Denmark Strait (about 2 Sv) is in the lower end of current estimates (e.g., Worthington 1970; Hopkins, 1991). The reason for the somewhat

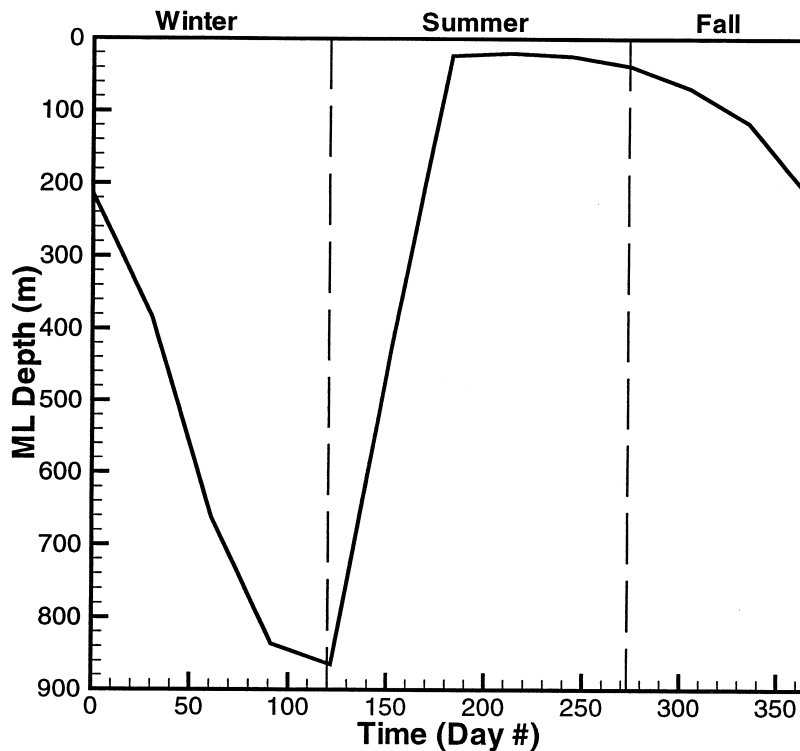


Fig. 3. The simulated annual cycle for the surface mixed layer thickness in the central Greenland Sea (75°N, 0°E). The winter, summer and fall periods are shown.

weak flow through the Denmark Strait is not clear, but could be linked to insufficient horizontal grid resolution in the strait, or that the climatological surface wind forcing fields is too weak.

The evolution of the simulated surface mixed layer depth in the central Greenland Sea at 75°N, 0°E is given in Fig. 3. Since the mixed layer depth reflects the integrated effect of input of buoyancy and turbulent kinetic energy into the surface waters, and consequently periods of stabilization and destabilization of the upper part of the water column, the year can be divided into three characteristic periods: Winter mixing period from January to April (day 1 to 120), summer stratification period from May to

September (day 121 to 273), and fall destabilization period from October to January (day 274 to 365).

4. Data

An extensive data set of C_T , collected from the years 1994 to 1997 within the ESOP1 and ESOP2 projects, have been used for the inorganic carbon budget calculation. The data were grouped into winter, summer and fall periods according to the definitions given above. Location of the sampling stations is shown for the winter and the summer period in Fig. 4a and b, respectively. The data set was also grouped into boxes surrounding the boundaries of

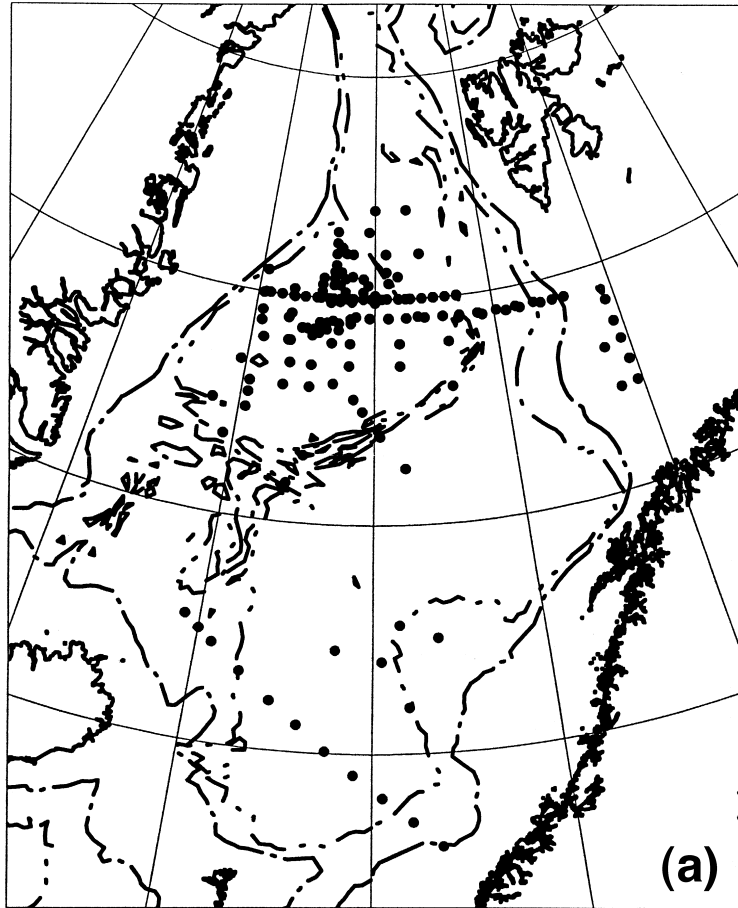


Fig. 4. (a) Location of the winter stations, (b) location of summer stations where data were collected during the expeditions 1994 to 1997.

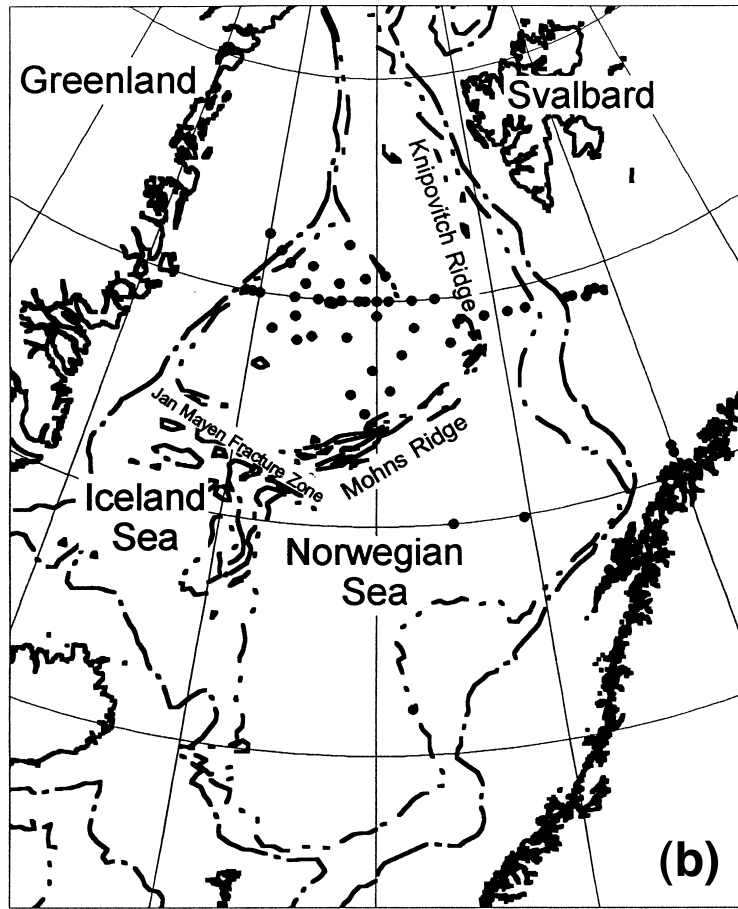


Fig. 4 (continued).

the Greenland Sea (Table 1) to represent the in and/or out flow of inorganic carbon through the

Table 1

Geographical boundaries of the boxes where the average measured C_T was taken to compute the flux of carbon *into* the Greenland Sea (a), and *out of* the Greenland Sea (b)

| | Boundary | Latitude (°N) | Longitude |
|-----|----------|---------------|-----------|
| (a) | 1 | 66–73 | 2°W–7°E |
| | 2 | 74.5–75 | 7°E–15°E |
| | 3 | 83–85 | 12°W–10°E |
| | 4 | 73–75 | 10°W–6°W |
| (b) | 1 | 73–74.5 | 5°W–7°E |
| | 2 | 75.5–76 | 0–6°E |
| | 3 | 75.5–77 | 0–4°E |
| | 4 | 73–75 | 10°W–6°W |

four boundaries. Complementary data representing the inflow from the Arctic Ocean through the Fram Strait was taken from the Swedish expedition in 1991 with the *IB Oden*. This data set was used for all three-time periods, thus ignoring possible seasonal variations in the C_T characteristics of water from the Arctic Ocean. As can be seen in Table 2, the coverage of the Greenland Sea and Norwegian Sea are sparser during the fall period (two cruises) than during the winter (five cruises) and summer (four cruises) periods. For this reason, the current study focuses on the winter and summer periods.

The interannual variation in the C_T data was investigated by plotting C_T for different years and look at the variation between years in comparison with variations within a year. As an example, C_T

Table 2

The cruises, study areas and the corresponding dates used in the calculations (GS, NS, AO are the Greenland Sea, the Norwegian Sea, and the Arctic Ocean, respectively)

| Vessel | Month | Year | Area | Time period |
|----------------------|-----------|------|-------|------------------------------------|
| <i>Håkon Mosby</i> | Feb–Mar | 1994 | GS | winter |
| <i>Håkon Mosby</i> | Feb–Mar | 1995 | GS,NS | winter |
| <i>Johan Hjort</i> | April–May | 1997 | GS,NS | winter |
| <i>Håkon Mosby</i> | Feb–Mar | 1997 | GS,NS | winter |
| <i>Johan Hjort</i> | April–May | 1995 | GS,NS | winter: 12 stns, summer: 9 stns |
| <i>IB Oden</i> | Aug–Sep | 1991 | AO | all periods |
| <i>Johan Hjort</i> | May–June | 1994 | GS,NS | summer |
| <i>James C. Ross</i> | July–Aug | 1996 | GS,NS | summer |
| <i>Johan Hjort</i> | Nov | 1995 | GS,NS | fall |
| <i>Håkon Mosby</i> | Nov–Dec | 1996 | GS | fall |

data plotted vs. depth for the box representing the outflow over Mohn's Ridge for 3 years — 1994, 1995 and 1997 — are shown in Fig. 5. Table 3 presents mean values and standard deviations for the winter period during the years 1994, 1995 and 1997, as well as the mean value and standard deviation for a sum of the 3 years independent of boxes and depth. From Fig. 5 and Table 3, it is clearly seen that it is not possible to detect any annual variation in the data set and that the standard deviation between years is in the same order as within a year. It is thus possible

to look at all years without taking the annual variation into consideration.

Mean values and standard deviations of C_T were calculated for the surface mixed layer and the 14 density layers of each box. The water transports from the model are averaged over the months representing the different periods and for each density layer.

Carbon transports could not be calculated for the fall period because of the few data points available for this time of the year.

5. Analytical methods

During all expeditions used in this investigation the sea water samples were collected with a rosette sampler and C_T was determined onboard within 24 h. The same method has been applied during all expeditions with minor differences. C_T was deter-

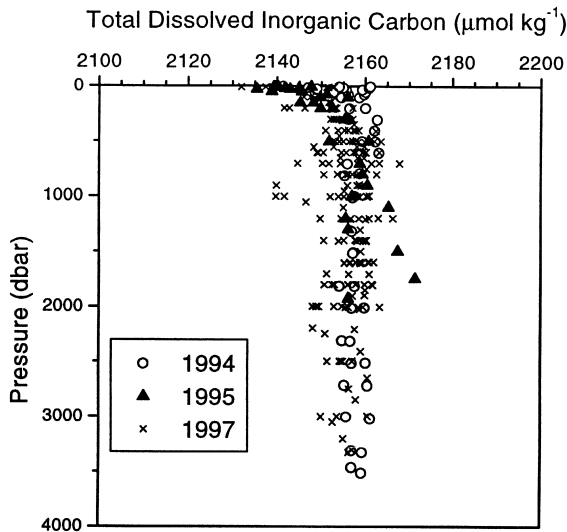


Fig. 5. Depth profiles of C_T for the years 1994, 1995 and 1997 representing the outflow over Mohn's Ridge.

Table 3

The intraannual and interannual mean value and standard deviation for all data during the winter period irrespective of box

| Year | Mean value and standard deviation ($\mu\text{mol kg}^{-1}$) | Number of data points |
|------|---|-----------------------|
| 1994 | 2153 ± 8 | 480 |
| 1995 | 2148 ± 10 | 431 |
| 1997 | 2153 ± 9 | 696 |
| Sum | 2152 ± 9 | 1607 |

mined by gas extraction from acidified sea water samples followed by coulometric titration with photometric detection (Johnson et al., 1985, 1987). The precision was obtained by replicate analysis of the samples. The accuracy was controlled by the use of certified reference material supplied by Andrew Dickson at Scripps Institution of Oceanography, USA. The values for C_T were corrected for the deviation from the certified value by using the ratio between the measured concentration and the certified concentration. The accuracy and precision for the C_T measurements varied between 1 and 2 $\mu\text{mol kg}^{-1}$ for each specific cruise.

To illustrate the variability of the entire data set the standard deviations of C_T within each depth layer was calculated. Fig. 6 shows the relative distribution for this variability within all density layers and boundaries illustrated in three intervals of standard deviation. From this figure, we see that during each cruise 31% of the data has a variability of less or equal to $\pm 4 \mu\text{mol kg}^{-1}$. These are the only data with a variability that is within the analytical precision and accuracy, which implies that the larger is more likely due to variations in horizontal distributions in the water column.

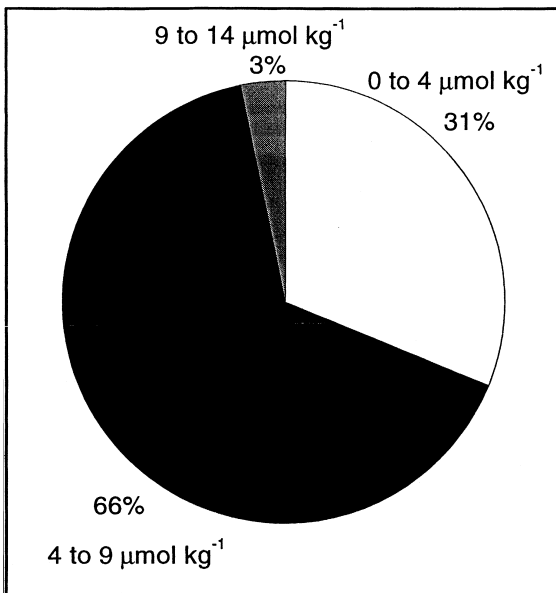


Fig. 6. The relative distribution of the C_T variability within the different density layers for all boundaries.

6. Carbon flux calculations

The carbon transports T_C (g yr^{-1}) have been obtained by multiplying the average flow F ($\text{m}^3 \text{s}^{-1}$) from the OGCM for a given time period with the mean total dissolved inorganic carbon concentration C_T (mol kg^{-1}) for each of the n density layers ($n = 1, \dots, 15$),

$$T_{C,n} = F_n C_{T,n} \rho_n m_C \alpha. \quad (1)$$

Here, ρ (kg m^{-3}) is the density of seawater, m_C (g mol^{-1}) is the atomic weight of carbon, and α (s yr^{-1}) denotes the number of seconds in a year.

In the following, the 15-density layers are collected into three water masses representing the major vertical stratification in the region: Layers 1–6 ($\sigma_\theta \leq 27.75$) represent the Surface Mixed Layer (SML), layers 7–11 ($27.86 \leq \sigma_\theta \leq 28.03$) represent the Intermediate Layer (IL), and layers 12–15 ($28.05 \leq \sigma_\theta \leq 28.09$) represent the Deep Layer (DL).

6.1. Error estimates

The magnitude of the errors in the carbon transports is determined by using Eq. (1) and calculating the resulting flux from the standard deviations $Sdev_n$ for the C_T values for each density layer n

$$Sdev = \left(\sum Sdev_n^2 \right)^{1/2} \quad (2)$$

The error estimates in the carbon flux for SML, IL, and DL were obtained by including the appropriate layers in Eq. (2).

It is important here to realize that the obtained error estimates only take into account the variability in the measured C_T values. Obviously, this uncertainty is only responsible for a part of the actual uncertainties in the calculations. For instance, temporal variations within the three-time periods are neglected in this study (not resolved by the observations, and probably not realistically simulated by the OGCM), and the same is the case for year-to-year variations in the coupled physical–biogeochemical system (neither resolved by the observations or the climatologically forced OGCM). Likewise, any spatial inhomogeneity along each of the four Greenland

Sea boundaries are neglected. Obviously, the obtained values of the carbon transport should be taken as a large scale mean.

Finally, it is essentially impossible to quantify the quality (or give an estimate of the error bars) of the simulated water transports due to the lack of flow observations in the region. The only transport estimates that can be used to determine the quality of the OGCM must rely on estimates of the flow over the ridges and through the channels surrounding the Nordic Seas. Such estimates are mostly deduced from hydrographic and tracer observations, and are by no means conclusive (Simonsen and Haugan, 1996).

7. Results

The inorganic carbon transport was calculated for summer and winter periods for each of the three depth layers and the four open boundaries. For the winter period January to April, Table 4a presents the mean water transports, the average C_T values for the in- and outflowing water, and the average carbon transport through the four boundaries and the three depth layers for the winter period. Table 4b shows the mean summer C_T values and the mean water transports. However, based on biological processes during summer, the dissolved inorganic carbon fluxes are accompanied by organic carbon fluxes. This made it unrealizable to attribute the inorganic carbon transport as the total carbon transport during this period. The standard deviations in the inorganic carbon transports are summarized according to Eq. (2) for the three depth layers. Furthermore, the net transports of water and inorganic carbon for the three depth layers in the Greenland Sea for the winter period are given in Table 5, and are obtained by taking the difference between the in- and outflux estimates in Table 4a. The standard deviation of C_T in the Greenland Sea during the winter period, for all depths and areas shows that the variability in C_T is $\pm 9 \mu\text{mol kg}^{-1}$ (Table 3) this implies that the approach with dividing data into boxes give rise to an uncertainty in the same magnitude as the total error in Table 5.

From Fig. 7 and Table 4a, it is seen that the main transport of carbon out of the Greenland Sea Basin

occurs in the SML through boundary 4. For the deeper layers, the main outflux occurs across the Mohn's Ridge and the Knipovich Ridge. The Arctic Ocean contributes with 36% of the carbon transported into the Greenland Sea mainly through the SML and the DL in the Fram Strait. Water flowing into the Greenland Sea through boundaries 1 and 2 is also one of the main contributors of carbon to the Greenland Sea, mainly in the SML and DL. The water in the DL is relatively old, modified deep water from the Atlantic and the Arctic Ocean. This dense water circulates in the Nordic Seas and has a high C_T content due to addition and dissolution of organic material, which can be one of the reasons for the large carbon flux in this layer into the Greenland Sea.

The results show a net transport of carbon out of the Greenland Sea during the winter season. The resulting difference gives a total net outflux of $0.024 \pm 0.006 \text{ Gt C yr}^{-1}$. Both the SML and the DL show a net influx, while there is an outflux in the IL. These results can be explained by that the Polar Water (PW) formed in the Arctic Ocean is transported into the Greenland Sea by the East Greenland Current. PW is a cold and relatively light water mass, and is found from the surface to approximately 150 m depth (Coachman and Aagaard, 1974; Johannessen, 1986). Part of this water will, after mixing with brine from sea ice formation, gain a higher density and can entrain to deeper layers. The net in-transport of carbon to the deep layers of the Greenland Sea can be explained by the high inflow of Eurasian Basin Deep Water (EBDW) from the Arctic Ocean through Fram Strait. Table 4a shows that the highest carbon transport into the deep Greenland Sea is through boundary 3, that is inflow of EBDW. We can also see that the SML stands for more than half of the water transport during the winter which is a result of the relatively deep surface mixed layer at this time of the year.

7.1. Uptake of carbon on an areal basis

As earlier described, the Greenland continental slope is included in our calculations. The Greenland Sea slope has an extensive ice cover, which affects the air–sea exchange of the region. By using the

Table 4

(a) The mean C_T values, water transports, and carbon fluxes for the in- and outflowing water through the four boundaries and for the three depth layers for the winter period. Also presented is the variability of the carbon concentration within the different boundaries, and the corresponding errors in the total transports

| | IN | | | OUT | | |
|------------|---|------------------------------|-----------------------------------|---|------------------------------|-----------------------------------|
| | Mean C_T ($\mu\text{mol kg}^{-1}$) | Mean water transport (Sv) | Carbon flux (Gt C yr $^{-1}$) | Mean C_T ($\mu\text{mol kg}^{-1}$) | Mean water transport (Sv) | Carbon flux (Gt C yr $^{-1}$) |
| <i>SML</i> | | | | | | |
| 1 | 2131 ± 6 | 1.772 | 1.470 ± 0.0002 | 2141 ± 5 | 0.421 | 0.351 ± 0.0003 |
| 2 | 2138 ± 5 | 2.088 | 1.738 ± 0.0007 | 2140 ± 3 | 1.841 | 1.533 ± 0.0002 |
| 3 | 2105 ± 8 | 2.402 | 1.965 ± 0.0013 | 2132 ± 10 | 0.870 | 0.721 ± 0.0022 |
| 4 | 2131 ± 14 | 0.651 | 0.540 ± 0.0001 | 2131 ± 14 | 3.535 | 2.927 ± 0.0029 |
| Σ | | 6.913 | 5.712 ± 0.002 | | 6.667 | 5.532 ± 0.004 |
| <i>IL</i> | | | | | | |
| 1 | 2147 ± 10 | 0.513 | 0.429 ± 0.0023 | 2150 ± 13 | 0.368 | 0.308 ± 0.0020 |
| 2 | 2148 ± 12 | 0.421 | 0.352 ± 0.0012 | 2150 ± 12 | 0.154 | 0.129 ± 0.0004 |
| 3 | 2147 ± 11 | 0.361 | 0.302 ± 0.0004 | 2162 ± 16 | 0.402 | 0.337 ± 0.0022 |
| 4 | 2140 ± 19 | 0.120 | 0.099 ± 0.0016 | 2143 ± 19 | 0.932 | 0.776 ± 0.0005 |
| Σ | | 1.414 | 1.182 ± 0.003 | | 1.856 | 1.550 ± 0.002 |
| <i>DL</i> | | | | | | |
| 1 | 2160 ± 7 | 0.982 | 0.826 ± 0.0003 | 2157 ± 8 | 1.395 | 1.172 ± 0.0006 |
| 2 | 2160 ± 11 | 1.188 | 0.999 ± 0.0003 | 2158 ± 10 | 1.702 | 1.430 ± 0.0011 |
| 3 | 2155 ± 9 | 1.725 | 1.447 ± 0.0012 | 2162 ± 10 | 0.313 | 0.264 ± 0.0005 |
| 4 | 2157 ± 10 | 0.071 | 0.060 ± 0.0002 | 2157 ± 10 | 0.359 | 0.302 ± 0.0005 |
| Σ | | 3.965 | 3.331 ± 0.001 | | 3.769 | 3.167 ± 0.001 |
| Total | | 12.292 | 10.225 ± 0.004 | | 12.292 | 10.249 ± 0.005 |

(b) The mean C_T values and water transports for the in- and outflowing water through the four boundaries and for the three depth layers for the summer period. Also presented is the variability of the carbon concentration within the different boundaries

| | IN | | OUT | |
|------------|---|------------------------------|---|------------------------------|
| | Mean C_T ($\mu\text{mol kg}^{-1}$) | Mean water transport (Sv) | Mean C_T ($\mu\text{mol kg}^{-1}$) | Mean water transport (Sv) |
| <i>SML</i> | | | | |
| 1 | 2080 ± 4 | 0.165 | 2042 ± 12 | 0.065 |
| 2 | 2115 ± 7 | 0.169 | 2064 ± 10 | 0.332 |
| 3 | 2105 ± 8 | 2.017 | 2071 | 0.946 |
| 4 | 2029 ± 10 | 0.154 | 2029 ± 10 | 1.749 |
| Σ | | 2.505 | | 3.092 |
| <i>IL</i> | | | | |
| 1 | 2148 ± 11 | 2.352 | 2138 ± 18 | 0.784 |
| 2 | 2149 ± 8 | 2.357 | 2143 ± 14 | 1.900 |
| 3 | 2147 ± 11 | 1.550 | 2122 ± 18 | 2.000 |
| 4 | 2135 ± 15 | 0.720 | 2135 ± 15 | 1.500 |
| Σ | | 6.979 | | 6.184 |
| <i>DL</i> | | | | |
| 1 | 2161 ± 7 | 1.053 | 2155 ± 8 | 0.826 |
| 2 | 2158 ± 3 | 1.045 | 2154 ± 12 | 1.208 |
| 3 | 2155 ± 9 | 1.352 | 2152 ± 3 | 1.565 |
| 4 | 2155 ± 10 | 0.104 | 2155 ± 10 | 0.163 |
| Σ | | 3.554 | | 3.762 |
| Total | | 13.038 | | 13.038 |

Table 5

A summary of the modeled net (IN minus OUT) water transports and the resulting carbon transports for the three depth layers during the winter situation

| Layer | Net transport of water (Sv) | Net Carbon flux (Gt C yr ⁻¹) |
|-------|-----------------------------|--|
| SML | 0.246 | 0.180 ± 0.005 |
| IL | -0.442 | -0.368 ± 0.004 |
| DL | 0.196 | 0.164 ± 0.001 |
| Total | 0.000 | -0.024 ± 0.006 |

ice-free area in the Greenland Sea during winter, the flux of carbon dioxide per square meter can be

calculated. The average ice area during winter is taken from the OGCM, and for an ice coverage > 40%, it amounts to $2.9 \cdot 10^{11}$ m². The total area of the Greenland Sea defined in our study is $5.6 \cdot 10^{11}$ m², yielding a total ice free area of $2.7 \cdot 10^{11}$ m², which agrees well with the reported ice free area from satellite images which reports areas of 2 to $4 \cdot 10^{11}$ m² (Gloersen et al., 1992). The flux of carbon amounts to $7.4 \text{ mol C yr}^{-1} \text{ m}^{-2}$, or $89 \text{ g C yr}^{-1} \text{ m}^{-2}$. A comparison with earlier reported values of $58 \text{ g C yr}^{-1} \text{ m}^{-2}$ (Johannessen et al., 1996) and the $40\text{--}80 \text{ g C m}^{-2} \text{ yr}^{-1}$ reported for the Nordic Seas (Walsh, 1989), indicates that our esti-

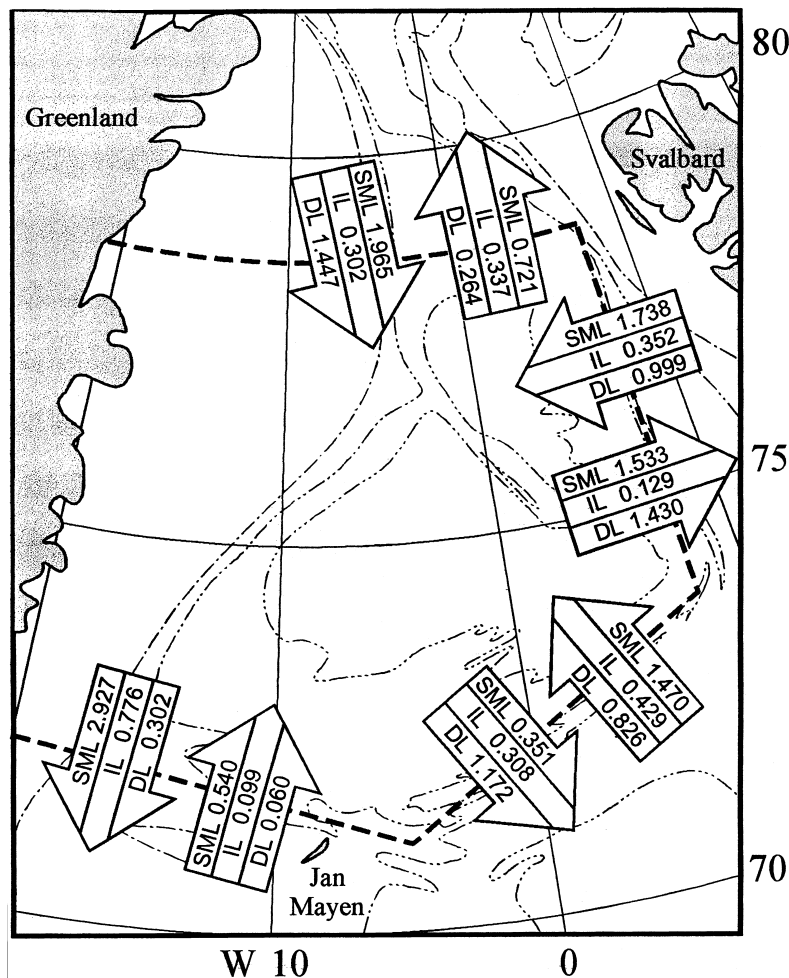


Fig. 7. The carbon flux through the four boundaries are shown for the three depth layers during the winter period. Arrows directed towards the Greenland Sea represent the influx of carbon, whereas arrows in the opposite direction represent the outflux of carbon. Numbers in the arrows denote the carbon transport in Gt C yr⁻¹ for the three depth layers.

mate is in the higher end of current estimates. However, the obtained value depends very much on the time of the year the estimates are representing, and how the area of the Greenland Sea is defined. It should be noted that estimates based on the in- and outflux of carbon in the Nordic Seas indicate an oceanic uptake of approximately $6 \text{ moles C yr}^{-1} \text{ m}^{-2}$ (Lundberg and Haugan, 1996), which agrees relatively well with our value for the Greenland Sea.

8. Discussion

In this work, one of the objectives was to study any inconsistencies when combining the modeled water transports with the in situ data on C_T . For a wintertime situation, the net transport of carbon required an uptake of $0.024 \pm 0.006 \text{ Gt C yr}^{-1}$, which agrees quite well with earlier reports. Lack of data during fall made any further calculation on the carbon transport impossible for this season. However, calculations for the inorganic carbon transport during the summer period have been performed.

The imbalance in the net flux of carbon from our calculations can be balanced by air–sea exchange, biological fixation of inorganic carbon, and/or sedimentation. The sedimentation of particulate organic carbon is a process that would contribute to the transport of carbon out of the system and would thus be a sink of carbon. Sedimentation is very closely related to biological production (Noji et al., 1996). The air–sea exchange could be both a source and a sink for the system. Since the winter period is before any biological production has taken place we have assumed the sedimentation to be negligible during this period. Thus, we attribute the imbalance in the net flux during wintertime to the air–sea exchange. The obtained imbalance require an oceanic uptake of carbon dioxide from the atmosphere by $0.024 \pm 0.006 \text{ Gt C yr}^{-1}$.

For comparison, the coupled physical–biogeochemical model of Drange (1996) with the ecosystem formulations of Fasham et al. (1990) and Broström and Drange (1998), give an oceanic uptake of 0.01 and $0.018 \text{ Gt C yr}^{-1}$, respectively. Furthermore, in a recent investigation based on a box model approach, Anderson et al. (1998b) obtained a value of $0.013 \text{ Gt C yr}^{-1}$ for the period 1990 to 1997. The

above studies reports CO_2 uptake based on annual fluxes, while the estimate from this study is based on a 4-month winter situation. Since the winter season is characterized by high wind speeds, intense cooling, and deep mixing, it seems realistic that our estimates are somewhat higher than other reported values.

During the summer period our calculations give a net flux of $0.22 \text{ Gt C yr}^{-1}$ into the Greenland Sea. It is here important to note that the computation is based on the flux of total dissolved inorganic carbon through the boundaries of the Greenland Sea, neglecting both dissolved and particulate organic carbon. Both sedimentation of carbon as particulate organic carbon and advection of organic material in particulate and dissolved form will transport carbon out of the system and therefore counteract the calculated influx of carbon. As the data representing inflow from the Arctic Ocean through the Fram Strait in this work does not show any seasonal signal, it is not affected by primary production, whereas the outflowing water through the Denmark Strait has been subject to formation of biological material. This will of course have an impact on the computed fluxes.

9. Conclusions

For the Greenland Sea region, we observe that the main influx of carbon is in the surface and deep waters, while the main outflux occurs in the intermediate layers. The resulting imbalance in the net flux of carbon requires an oceanic uptake of $0.024 \pm 0.006 \text{ Gt C yr}^{-1}$ during winter. This implies that the Greenland Sea acts as a sink of atmospheric carbon dioxide during this time of the year. We can also conclude that it is only possible to evaluate the air–sea exchange of carbon dioxide during the winter period when the biological production is negligible.

The $0.024 \pm 0.006 \text{ Gt C yr}^{-1}$ uptake of carbon in the Greenland Sea obtained in this study is higher than the estimates found in the literature. One plausible reason for this is that our estimate is based on the months January to April, characterized by high wind speeds and intense cooling of the surface water, whereas the other estimates are annual mean values.

In fact, Anderson et al. (1998b) show that the air–sea flux of carbon is highest during the winter months.

Earlier reports estimate the oceanic uptake of CO₂ in the Nordic Seas to 0.05 (Lundberg, 1994) and 0.06 Gt C yr⁻¹ (Drange, 1996). This implies that the Greenland Sea is responsible for an oceanic uptake of around 45% of the entire Nordic Seas uptake, based on the oceanic uptake of CO₂ obtained in this study.

Finally, it should also be mentioned that this investigation gives the total uptake of carbon dioxide, and that it does not say anything about how much anthropogenic carbon dioxide is sequestered in the Greenland Sea region. One reported value of the sequestering of anthropogenic carbon dioxide below 1500 m in the Greenland Sea is 0.0024 ± 0.0007 Gt C yr⁻¹ (Anderson et al., 1998a). Comparing this to our computed oceanic uptake, indicates that up to 10% is of anthropogenic origin and that it may be sequestered below 1500 m.

Acknowledgements

This work has been supported by the Nordic Council of Ministers and by the Commission of the European Union under the contract MAS3-CT95-0015 of the Mast-3 programme. The Swedish Natural Research Council and the Marine Research center in Göteborg, Sweden has also contributed to this work. The OGCM model simulations have been supported by the Programme of Supercomputing under the Norwegian Research Council. Many thanks to Kim Holmén, University of Stockholm, for constructive criticism and discussions during the production of the manuscript and to Göran Broström, University of Göteborg. We also thank NORFA for contributing to many inspiring and developing meetings.

References

- Aagaard, K., Fahrbach, E., Meincke, J., Swift, J.H., 1991. Saline outflow from the Arctic Ocean: its contribution to the deep waters of the Greenland, Norwegian and Iceland Seas. *J. Geophys. Res.* 96, 20433–20441.
- Anderson, L.G., Chierici, M., Fogelqvist, E., Johannessen, T., 1998a. Flux of anthropogenic carbon into the deep Greenland Sea. *J. Geophys. Res.*, Special Volume to Maurice Ewing Symposium papers. Accepted.
- Anderson, L.G., Drange, H., Fransson, A., Chierici, M., Skjelvan, I., Johannessen, T., Rey, F., 1998b. Annual variability of carbon flux in the upper Greenland Sea, as evaluated from measured data and a box model. *Tellus*, manuscript in preparation.
- Bleck, R., Rooth, C., Hu, D., Smith, L.T., 1992. Salinity-driven thermohaline transients in a wind- and thermohaline-forced isopycnic coordinate model of the North Atlantic. *J. Phys. Oceanogr.* 22, 1486–1515.
- Bönisch, G., Blindheim, J., Bullister, J.L., Schlosser, P., Wallace, D.W.R., 1997. Longterm trends of temperature, salinity, density, and transient tracers in the central Greenland Sea. *J. Geophys. Res.* 102, 18553–18571.
- Broecker, W.S., 1991. The Great Ocean Conveyor. *Oceanography* 4 (2), 79–89.
- Broström, G., Drange, H., 1998. On the mathematical formulation of the marine plankton system. *Sarsia*, submitted.
- Buch, E., Hansen, B., Johannessen, J.A., Malmberg, S., Østerhus, S., 1988. The exchange of water and heat between the Atlantic and the Nordic Seas. Document presented to the International WOCE Scientific Conference, Paris, Nov. 28–Dec. 2, 1988.
- Coachman, L.K., Aagard, K., 1974. Physical oceanography of Arctic and Subarctic Seas. In: Herman, Y. (Ed.), *Marine Geology and Oceanography of the Arctic Seas*. Springer-Verlag, New York, pp. 1–72.
- Dickson, R.R., Brown, J., 1994. The production of North Atlantic Deep Water: sources, rates and pathways. *J. Geophys. Res.* 99, 12319–12341.
- Drange, H., 1996. A 3-dimensional isopycnic coordinate model of the seasonal cycling of carbon and nitrogen in the Atlantic Ocean. *Phys. Chem. Earth* 21, 503–509.
- Drange, H., Simonsen, K., 1997a. Formulation and spin-up of the ESOP2 version of MICOM. Technical Report No. 117. Nansen Environmental and Remote Sensing Center.
- Drange, H., Simonsen, K., 1997b. Formulation of air–sea fluxes in the ESOP2 version of MICOM. Technical Report No. 125. Nansen Environmental and Remote Sensing Center.
- Fasham, M.J.R., Ducklow, H.W., McKelvie, S.M., 1990. A nitrogen-based model of plankton dynamics in the oceanic mixed layer. *J. Mar. Res.* 48, 591–639.
- Gloersen, P., Campbell, W.J., Cavalieri, D.J., Comiso, J.C., Parkinson, C.L., Zwally, H.J., 1992. Arctic and Antarctic sea ice, 1978–1987: satellite passive-microwave observations and analysis. *NASA SP-511*. NASA, Washington, DC, 290 pp.
- Gruber, N., Sarmiento, J.L., Stocker, T.F., 1996. An improved method for detecting anthropogenic CO₂ in the oceans. *Global Biogeochem. Cycles* 10 (4), 809–837.
- Hopkins, T.S., 1991. The GIN Sea — a synthesis of its physical oceanography and literature review 1972–1985. *Earth Sci. Rev.* 30 (3–4), 318.
- Hurrell, J.W., 1995. Decadal trends in the North Atlantic Oscillation: regional temperatures and precipitation. *Science* 269, 676–679.
- Huschke, R.E., 1969. Arctic cloud statistics from air calibrated

- surface weather observations. Memo.-5003-PR, Rand Corp. Santa Monica, CA.
- Johannessen, O.M., 1986. Brief overview of the physical oceanography in the Nordic Seas. In: Hurdle, B.G. (Ed.), Springer-Verlag, New York, pp. 103–127, Chap. 4.
- Johannessen, T., Skjelvan, I., Miller, L., Stoll, M.H.C., Jansen, E., Anderson, L.G., 1996. Air/sea fluxes of carbon in the Nordic Seas with emphasis on the Greenland Sea. In: Wadhams, P., Wilkinson, J.P., Wells, S.C.S. (Eds.), European Subpolar Ocean Programme 2, pp. 491–503.
- Johnson, K.M., King, A.E., Sieburth, J.M., 1985. Coulometric TCO_2 analyses for marine studies: an introduction. *Mar. Chem.* 16, 61–82.
- Johnson, K.M., Sieburth, J.M., Williams, P.J., Brandstrom, L., 1987. Coulometric total carbon dioxide analysis for marine studies: automation and calibration. *Mar. Chem.* 21, 117–133.
- Legates, D.R., Willmott, C.J., 1990. Mean seasonal and spatial variability in gauge-corrected, global precipitation. *Int. J. Climatol.* 10, 111–127.
- Levitus, S., Boyer, T.P., 1994. In: World Ocean Atlas 1994 Volume 4: Temperature. NOAA Atlas NESDIS 4, Washington, DC, p. 117.
- Levitus, S., Burgett, R., Boyer, T.P., 1994. In: World Ocean Atlas 1994 Volume 3: Salinity. NOAA Atlas NESDIS 3, Washington, DC, p. 99.
- Lundberg, L., 1994. CO_2 air–sea exchange in the Nordic Seas. An attempt to make an estimate based on data. *Oceanologica Acta* 17 (2), 159–175.
- Lundberg, L., Haugan, P.M., 1996. A Nordic Seas–Arctic Ocean carbon budget from volume flows and inorganic carbon data. *Global Biogeochem. Cycles* 10, 493–510.
- Maier-Reimer, E., Hasselmann, K., 1987. Transport and storage of CO_2 in the ocean — an inorganic ocean-circulation carbon cycle model. *Climate Dynamics* 2, 63–90.
- Maykut, G.A., 1978. Energy exchange over young sea ice in the Central Arctic. *J. Geophys. Res.* 83, 3646–3658.
- Meincke, J., 1983. The modern current regime across the Greenland–Scotland Ridge. In: Bott, Saxov, Talwani, Thiede (Eds.), Structure and Development of the Greenland–Scotland Ridge. Plenum Publishing Corporation, pp. 637–650.
- Nansen, F., 1906. Northern Waters: Captain Roald Amundsen's Oceanographic Observations in the Arctic Seas on 1901. Vid. Selskap Skrifter I. Mat. Naturv. Kl. Dybwad, Christiania 1 (3).
- New, A.L., Bleck, R., Jia, Y., Marsh, R., Huddleston, M., Bernard, S., 1995. An isopycnic model study of the North Atlantic: Part I. Model experiment. *J. Pol. Oceanogr.* 25, 2679–2711.
- Noji, T.T., Rey, F., Miller, L., Børshheim, K.Y., Hirche, H.-J., Urban-Rich, J., 1996. Plankton dynamics and sedimentation. In: Wadhams, P., Wilkinson, J.P., Wells, S.C.S. (Eds.), European Subpolar Ocean Programme 2, pp. 540–554.
- Oberhuber, J.M., 1988. The budgets of heat, buoyancy and turbulent kinetic energy at the surface of the global ocean. In: Tech. Rep. 15 Max-Planck Institut für Meteorologie, Hamburg, Germany.
- Quay, P.D., Tilbrook, B., Wong, C.S., 1992. Oceanic uptake of fossil fuel CO_2 : carbon-13 evidence. *Science* 256, 74–79.
- Sarmiento, J.L., Orr, J.C., Siegenthaler, U., 1992. A perturbation simulation of CO_2 uptake in an ocean general circulation model. *J. Geophys. Res.* 97, 3621–3645.
- Schlosser, P., Böhmisch, G., Rhein, M., Bayer, R., 1991. Reduction of deep water formation in the Greenland Sea during the 1980s: evidence from tracer data. *Science* 251, 1054–1056.
- Siegenthaler, U., Sarmiento, J.L., 1993. Atmospheric carbon dioxide and the ocean. *Nature* 365, 119–125.
- Simonsen, K., Drange, H., 1997. Surface forcing and initialization of the ESOP2 version of MICOM. Technical Report No. 116. Nansen Environmental and Remote Sensing Center.
- Simonsen, K., Haugan, P.M., 1996. Heat budgets of the Arctic Mediterranean and sea surface heat flux parameterizations for the Nordic Seas. *J. Geophys. Res.* 101, 6553–6576.
- Suess, H.E., 1955. Radiocarbon concentration in modern wood. *Science* 122, 415–417.
- Swift, J.H., Koltermann, K.P., 1988. The origin of Norwegian Sea deep water. *J. Geophys. Res.* 93, 3563–3569.
- Takahashi, T., Olafsson, J., Goddard, J.G., Chipman, D.W., Sutherland, S.C., 1993. Seasonal variation of CO_2 and nutrients in the high-latitude surface oceans: a comparative study. *Global Biogeochem. Cycles* 7, 843–878.
- Takahashi, T., Takahashi, T.T., Sutherland, S.C., 1995. An assessment of the role of the North Atlantic as a CO_2 sink. In: Eglinton, G., Elderfield, H., Whitfield, M., Williams, P.J.LeB. (Eds.), The Role of the North Atlantic in the Global Carbon Cycle. Philosophical Transactions: Biological Sciences 348, pp. 1431–1438.
- Walsh, J.J., 1989. Arctic carbon sinks: present and future. *Global Biogeochem. Cycles* 3 (4), 393–411.
- Worthington, L.V., 1970. The Norwegian Sea as a Mediterranean Basin. *Deep-Sea Res.* 17, 77–84.